Vol. 3(1), pp. 1-20, Sept 2024
eISSN 2976-4009

ASEAN Journal of Process Control

Research Article

Performance Evaluation of Unconventional Index for Controllability and Stability Analysis: Application on a Patented Reactor for Renewable Hydrogen Production

Noraini Mohd[1*], Jobrun Nandong[2]

[1] School of Energy and Chemical Engineering, Xiamen University Malaysia, 43900 Sepang, Selangor Darul Ehsan, MALAYSIA

[2] Department of Chemical Engineering, Curtin University Malaysia, Miri 98009, Sarawak, MALAYSIA

*Corresponding Author: noraini.mohd@xmu.edu.my

Academic Editor: Dr Mohd Farid bin Atan

Abstract: In a decentralised PID control, improper input-output pairings would reduce plant safety, productivity, and profitability. When designing a process control system, controllability evaluation is crucial since it helps to pinpoint the best input-output combinations. Current conventional indices, however, are unable to determine the highest possible closed-loop efficiency. Using MATLAB software, this study proposes an innovative index to simultaneously find control pairings and maximum control performance. The index, namely Loop Gain Controllability (LGC) index was evaluated on a distillation process and integrating tank before being used to study a patented industrial-scale reactor's controllability and stability. The LGC index provided values of 1.39, 1.45, 1.40, and 1.08 for four reactor schemes when applied to a decomposition reactor for hydrogen production, while RGA and NI proposed values of 1 for the first three schemes (direct pairing) and negative for the fourth plan (inverse pairing). The closed-loop control response of reactor scheme 2 (P2), which demonstrated that it was controllable and stable when simulated, proved the hypothesis that the larger the LGC value would lead to higher controllability and stability. This demonstrates that LGC can simultaneously analyse control system stability, something that standard indices are unable to achieve.

Keywords: Controllability Index, Decentralized PID, MATLAB Simulation, Renewable Hydrogen

1. Introduction

Many industrial processes are multivariable and controlled by decentralised PID. Multivariable processes are complex to control depending on their controllability. This controllability characteristic depends on the system design and intrinsic process, which can cause complicated dynamics including nonminimum-phase, long-time delays, unstable poles, and process interactions. In multivariable processes, one input variable often affects numerous output variables. To achieve excellent closed-loop performance, a decentralised PID control system must include process interactions. Due to process interactions, most PID controller tuning approaches for single-input, single-output (SISO) processes difficult to be used to multivariable processes. When the interaction limits control efficiency, decentralised PID control is difficult to use for multivariable processes with substantial interaction effects. A number

of existing controllability indices, such as the Relative Gain Array (RGA) [1], Niederlinski Index (NI) [2], dynamic RGA (DRGA), and relative normalised gain array (RNGA), may be employed to determine the degree of the process interaction.

Within the last three decades, developments in process controller technology have allowed for better utilisation of process dynamics, which has led to enhanced process operation [4–8]. Process controller design has also revived interest in improving controllability methods that account for process dynamics. To apply an acceptable control strategy, one must analyse a system's process controllability. It may be essential to redesign a system with low controllability for easier control. Alternatively, a sophisticated control technique could control a poorly controllable system that cannot be modified. Designing and controlling any process system requires process controllability techniques. The present or conventional controllability analysis techniques can be categorised into three broad groups: (a) steady-state, (b) model-based linear dynamic, and (c) model-based nonlinear dynamic [3]. The steady-state RGA, determined by utilising the open-loop gains of the provided process model, represents one of the most commonly used indices for evaluating process controllability [1]. Process interaction's effect on controllability can be assessed easily using it. Careful input-output pairing in the decentralised control system helps avoid poor controllability. It is suggested, when undertaking decentralised controller pairing selection based on the RGA analysis, to match the manipulated variable uj with the controlled variable yi such that the RGA element (λij) is positive and as close to unity as possible. For decades, the steady-state RGA has been utilised in the process sector to find controller pairings that avoid weak controllability due to its simplicity. There are more complex controllability approaches, but the RGA-based method is still used as an initial screening tool to prevent pairings that are impractical based on dependability and robustness [9]. According to the viewpoint of the RGA, the optimal pairings ought to adhere to two rules: (a) the pairings across the diagonal RGA ought to have components that are close to unity at frequencies near the closed-loop bandwidth; and (b) the steady-state RGA components must be positive (avoid pairings with negative elements if feasible). Notably, multiple variations of Bristol's RGA were created, including the DRGA and RNGA. Shen and co-workers [10] introduced an in-depth analysis and discussion of the controllability of a process, as well as a few guidelines for input-output coupling in a decentralised control system:

a) All paired RGA elements should be positive.
b) Niederlinski Index (NI) should be positive.
c) All paired RNGA elements should be as close as possible to 1.
d) Large RNGA elements should be avoided.

The findings of the controllability evaluation using RNGA, RGA, and NI criteria according to the rules which explain the decentralised control design's controllability problem. As stated by Shen et.al., (2010) [10], the RNGA is employed to assess loop interactions, whereas the RGA and NI are employed to filter out unfeasible pairings that can result in unstable closed-loop behaviours. Similarly, to the RGA criterion, the NI index is able to be used independently to determine controller pairings in a decentralised control system. Nevertheless, this provides a shallow comprehension of the challenge of controllability concerned.

Should a specific controllability index can offer the utmost attainable performance, ultimately the decentralised PID control system could be tuned with greater accuracy. If the utmost attainable control performance with decentralised PID control is unsatisfactory an even more advanced control strategy can be selected for consideration. It is important to remember that the input-output pairing selection and controller tuning make significant contributions to the closed-loop performance and robustness. An enhanced controllability analysis ought to offer: (a) correct input-output pairings in the event of process interactions; and (b) a projection of the maximum attainable controller performance. However, none of the previously mentioned controllability indices can simultaneously fulfil both of these requirements. In addition, the majority of existing controllability assessment techniques only consider controller pairings according to steady-state process gains, i.e. they disregard the impact of time delays and time constants.

Thus, there is a deficiency in the effective utilisation of both steady-state and dynamic process data for enhancing decentralised control design especially for nonlinear process [11].

In light of this deficiency, the primary objective of this study is to develop a comprehensive controllability analysis using an unconventional index named as Loop Gain Controllability (LGC) index. The proposed LGC

considers both the steady-state and dynamic behaviours of the particular process to be taken into account which includes (a) process time constants, (b) time delays, and (c) process interactions. This index is anticipated to offer greater insight into the effect of process interactions, time delays, and time constants on the controllability of a two-input and two-output (TITO) process.

2. Loop Gain Controllability (LGC) Index

2.1. Fundamental of LGC

The purpose of the LGC index is to determine the controllability of a process according to a given process model, in which controllability is represented by an index value which is labelled as, δ. The principle behind LGC is to establish a controllability index by combining information from the controller and process model. Figure 1 depicts the block diagram of a typical single-loop feedback control structure. The dashed area in Figure 1 represents the proposed LGC computation. In this study, the LGC index is derived for a model with two inputs and two outputs (TITO) and tested via the MATLAB environment. It should be pointed out that this method can be extended to multivariable processes with higher dimensions.

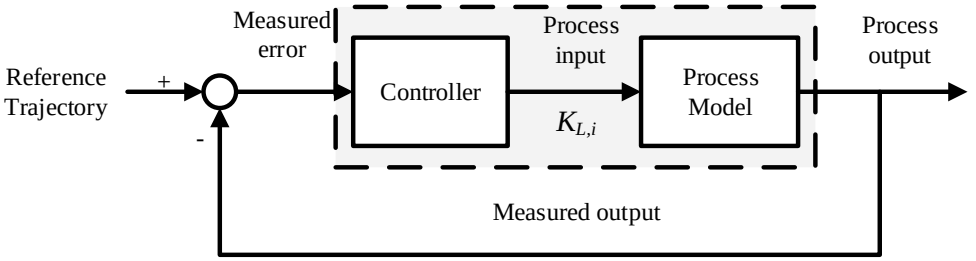

Figure 1: LGC calculation (dashed square area) of a feedback control loop structure.

In a decentralized control system, the LGC index is specified by the variance between the minimum upper limit ($\overline{K}_{i,min}$) and the maximum lower limit ($\underline{K}_{i,max}$) on the particular loop gain, i.e., $K_{L,i} = K_{c,i}k_{eff,ii}$ where $K_{c,i}$ and $k_{eff,ii}$ represent the controller gain and effective open-loop process gain correspondingly for the ith control loop. To guarantee closed-loop stability, the loop gain value needs to be positioned in the range of

$$\underline{K_{i,max}} < K_{L,i} < \overline{K}_{i,min} \quad (1)$$

Figure 2 shows the key notion of LGC index calculation based on the equation (2). With the PID controller, a process might demonstrate numerous upper and lower limits on the loop gain [11]. The distance between the minimum upper and maximum lower limits embodies the LGC index. For the TITO process, the LGC computations comprise finding the minimum upper limit $\overline{K}_{i,min}$ and maximum lower limit $\underline{K}_{i,max}$ for both control loops distinctly. For the ith-loop, the LGC index δ_i

$$\delta_i = \overline{K}_{min} - \underline{K}_{max}, for\ \underline{K}_{max} > 0 \quad (2)$$

else,

$$\delta_i = \overline{K}_{min}, for\ \underline{K}_{max} < 0 \quad (3)$$

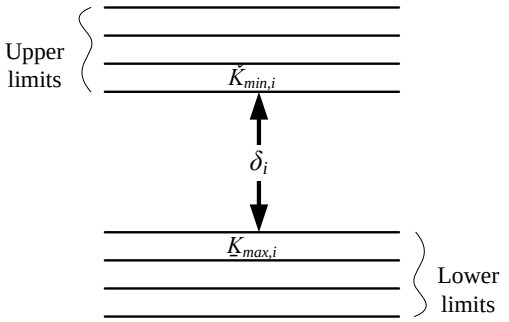

Figure 2: Upper and lower limits concepts undermine the LGC calculation.

A bigger value of δ_i infers a greater robustness boundary as well as a greater maximum attainable performance of the particular PID control system. In a SISO case, if the First Order plus Deadtime (FOPDT) model is utilized to represent the process dynamics, the LGC index is represented as a function of the process gain k, time θ, and time constant τ, thus,

$$\delta_i = f(k, \theta, \tau) \tag{4}$$

It must be noted that for a multivariable process, the LGC index means to be a function of the process interaction in addition to the process gains, deadtimes and time constants. The next section explains how the LGC index for the TITO procedure was derived.

2.2 The Development of The LGC Index

Based on the developed EOTF (see Appendix), the closed-loop setpoint transfer function for loop 1 is

$$H_{R_1}(s) = \frac{g_{c_1}(s) g_1^{eff}(s)}{1 + g_{c_1}(s) g_1^{eff}(s)} \tag{5}$$

By assuming the dead time term with the first-order Padé formula and presuming the use of a P-only controller, the closed-loop characteristic equation that corresponds to equation (10) can be derived.

$$1 + \frac{K_{L_1}(\tau_{I_1} s + 1)}{\tau_{I_1} s} \left\{ \frac{1 - \alpha_{11} s}{(\tau_{11} s + 1)(\alpha_{11} s + 1)} - \psi_1 \left[\frac{(1 - \alpha_{I_1} s)(\tau_{22} s + 1)}{(\tau_{12} s + 1)(\tau_{21} s + 1)(\alpha_{I_1} s + 1)} \right] \right\} = 0 \tag{6}$$

where $\alpha_{ii} = 0.5\theta_{ii}$; the loop gain is $K_{L_1} = k_{c_1} k_{11}$ where k_{c1} is the controller gain.

The characteristic equation (15) can be written in a specific polynomial form as:

$$f_6 s^6 + \left(f_5 + K_{L_1} h_5\right) s^5 + \left(f_4 + K_{L_1} h_4\right) s^4 + \left(f_3 + K_{L_3} h_3\right) s^3 + \cdots$$
$$\left(f_2 + K_{L_2} h_2\right) s^2 + \left(f_1 + K_{L_1} h_1\right) s + K_{L_1} h_0 = 0 \tag{7}$$

For the parameters in (16), one may write the general expressions as in equation (17),

$$f_k = (a_{k-2}\tau_{11} + a_{k-1})\tau_{I_1} \quad for \quad k = 1,2, \ldots 6 \tag{8}$$
$$h_k = \tau_{I_1}\left(b_{1(k-1)} - \psi_1 b_{2(k-1)}\right) + b_{1k} - \psi_1 b_{2k}$$

$$for\ k = 0,1, \ldots 5 \tag{9}$$

The comprehensive list of parameters listed in (16) to (18) can be found in the Appendix. By employing the PID stability theory in [13], it is possible to derive upper and lower limits for the loop gain. Taking into account the concept of upper and lower limits, the value of the LGC index, such as for loop 1, δ_1 is calculated as in equation (2) or (3).

In this investigation, the LGC index is computed using a P-only controller. One may also calculate the LGC index for the PI or PID controller using the same method, however, this will result in a higher-order characteristic polynomial (seventh order for PI and eighth order for PID). It ought to be noted that the LGC index developed in this study is only applicable when the effective deadtime is $\theta_{I_i} > 0$; otherwise, the procedure above is not applicable, i.e., for $\theta_{I_i} < 0$.

If $\theta_{I_i} > 0$, the following interpretations of the δ_i value can be made:

a) A positive δ_i value indicates the selected pairing is controllable. If $\delta_i \leq 0$ then the loop is uncontrollable using the PID control (or very difficult to control).
b) A larger δ_i value means a greater maximum achievable control performance of the given pairing.
c) If two systems have comparable values of the LGC index, then the controllability performance of the two systems should also be comparable, even though the systems have different orders, e.g., one first-order and another fourth-order.
d) The LGC index may be additionally calculated using the FOPDT model (6) in the case of a single loop. By estimating the dead time term with the Padé formula of the first order, it is demonstrated that the LGC index according to g_{ii} can be determined by

$$\delta_{ii} = \frac{\tau_{ii}+0.5\theta_{ii}}{0.5\theta_{ii}} \quad (10)$$

The procedure for determining the LGC index of a particular system, which includes the application of LGC in a closed-loop MATLAB simulation, is depicted in Figure 3.

3. Evaluation of LGC On Distillation Column and Interacting Tanks

This section describes how to apply LGC analysis to two common processes: benzene-toluene separation and liquid-interacting vessels. The programme Control Station Loop-Pro Trainer simulates both TITO procedures. A single-direction step response test with a 10% nominal value change yields the transfer functions depicted in Tables 1 and 2. To determine controllability, all LGC index models are evaluated. In addition, standard RGA and NI indices are employed to compare controllability. To assess closed-loop performance against the Integral Absolute Error (IAE) benchmark, a linearized model-based simulation is run.

Table 1: Baseline conditions for the distillation column

Parameters	Value
Reflux R (%) = u1	50
Steam S (%) = u2	47
Feed flow (kg/min)	596
Top purity, Xd (%) = y1	94.5
Bottom purity, Xb (%) = y2	2.6%

Table 2: Baseline conditions for the interacting tanks

Parameters	Value
Feed flow 1 (m^3/min) = u1	61.5
Feed flow 2 (m^3/min) = u2	61.5
Disturbance 1 (m^3/min)	1.0
Liquid Level 1 (m) = y1	3.46
Liquid Level 2 (m) = y2	3.26

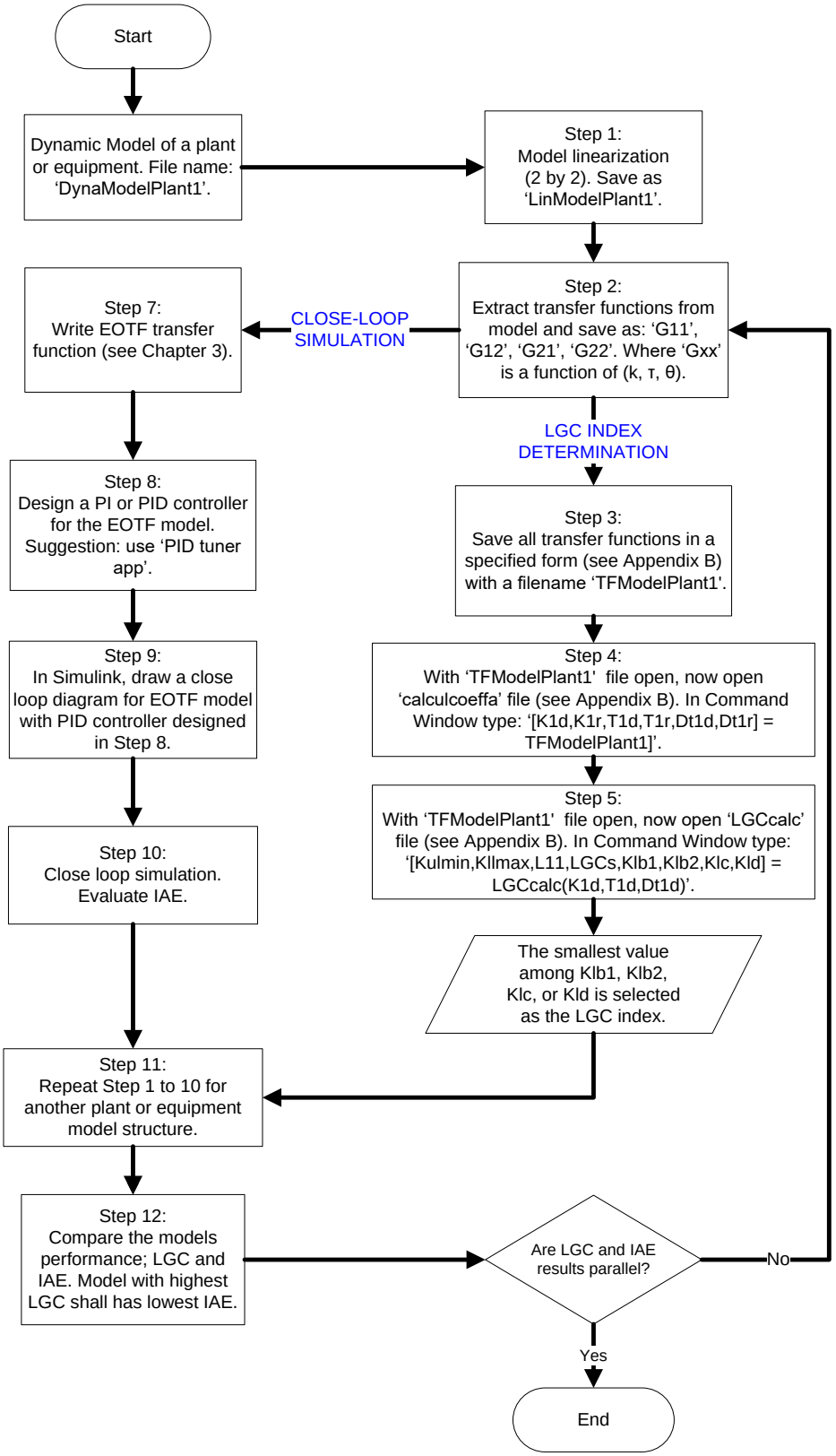
Start
Dynamic Model of a plant or equipment. File name: 'DynaModelPlant1'.
Step 1: Model linearization (2 by 2). Save as 'LinModelPlant1'.
Step 2: Extract transfer functions from model and save as: 'G11', 'G12', 'G21', 'G22'. Where 'Gxx' is a function of (k, τ, θ).
CLOSE-LOOP SIMULATION
Step 7: Write EOTF transfer function (see Chapter 3).
LGC INDEX DETERMINATION
Step 3: Save all transfer functions in a specified form (see Appendix B) with a filename 'TFModelPlant1'.
Step 4: With 'TFModelPlant1' file open, now open 'calculcoeffa' file (see Appendix B). In Command Window type: '[K1d,K1r,T1d,T1r,Dt1d,Dt1r] = TFModelPlant1]'.
Step 5: With 'TFModelPlant1' file open, now open 'LGCcalc' file (see Appendix B). In Command Window type: '[Kulmin,Kllmax,L11,LGCs,Klb1,Klb2,Klc,Kld] = LGCcalc(K1d,T1d,Dt1d)'.
The smallest value among Klb1, Klb2, Klc, or Kld is selected as the LGC index.
Step 8: Design a PI or PID controller for the EOTF model. Suggestion: use 'PID tuner app'.
Step 9: In Simulink, draw a close loop diagram for EOTF model with PID controller designed in Step 8.
Step 10: Close loop simulation. Evaluate IAE.
Step 11: Repeat Step 1 to 10 for another plant or equipment model structure.
Step 12: Compare the models performance; LGC and IAE. Model with highest LGC shall has lowest IAE.
Are LGC and IAE results parallel?
No
Yes
End

Figure 3: The overall methodology of LGC index determination and closed-loop simulation.

3.1. Distillation Column

The first example comes from the binary distillation column that separates benzene and toluene. This study used Control Station Loop-Pro to simulate distillation columns. Due to intensive nonlinear dynamics, an advanced model-based controller may be better for distillation column (DC) control in some cases [14]. However, many distillation operations still use the standard multi-loop PID control method due to its simplicity and reliability. Thus, before choosing a controller, the distillation process must be assessed for controllability.

The following section evaluates the distillation process's controllability using the LGC index. LGC analysis uses dynamic process information, hence a linearized model is needed. Under nominal operating conditions, the step response test determines the model. Due to nonlinearity, the distillation column step-up and step-down linearized models with equivalent perturbations are not identical, as shown in Table 3. LGC analysis is utilised in both the single-loop and multi-loop situations. The LGC index computations for the single-loop case rely on the given first-order transfer functions g_{11} (loop 1) and g_{22} (loop 2) independently. In the case of multiple loops, equation (8) yields two EOTFs, one for loop 1 and another for loop 2. After estimating the delay terms with Padé approximations of the first order, both EOTFs are simplified into the form of a fifth-order transfer function. Note that both EOTFs are formed through direct coupling configurations. The LGC index computations are performed independently for each EOTF, i.e., one for each cycle. Table 4 displays the LGC index, RGA, and NI values.

Table 3: Transfer Functions for the DC and IT processes.

Model	g_{11}	g_{12}	g_{21}	g_{22}
Distillation model by step-up test: Model 1	$\frac{0.415e^{-22.4s}}{41.9s+1}$	$\frac{-0.919e^{-24.8s}}{43.2s+1}$	$\frac{1.049e^{-44.6s}}{63.2s+1}$	$\frac{-0.161e^{-7.6s}}{28.7s+1}$
Distillation model by step-down test: Model 2	$\frac{1.056e^{-32.6s}}{36.2s+1}$	$\frac{-0.333e^{-18.7s}}{40.7s+1}$	$\frac{0.146e^{-21.7s}}{21.7s+1}$	$\frac{-0.984e^{-31.7s}}{60.9s+1}$
Interacting tanks by step-up test: Model 3	$\frac{0.0755e^{-5.91s}}{16.4s+1}$	$\frac{0.042e^{-6.75s}}{15s+1}$	$\frac{0.0361e^{-6.77s}}{17.1s+1}$	$\frac{0.0767e^{-7.57s}}{16.1s+1}$
Interacting tanks by step-down test: Model 4	$\frac{0.0673e^{-6.11s}}{13.7s+1}$	$\frac{0.0404e^{-5.95s}}{14.2s+1}$	$\frac{0.034e^{-6.84s}}{14.9s+1}$	$\frac{0.0697e^{-6.81s}}{14.6s+1}$

Table 4: Distillation Column Step-Up Model 1: values of RGA, NI and LGC indices

Step Up Control Loop	**Single Loop: 1st Order Model**			**Multi-Loop: 5th Order (EOTF) Model**				
	LGC	PI controller	IAE	LGC	PI controller	IAE	RGA	NI
Loop 1, g_{11}	4.74	$K_{c1} = 2.262$ $\tau_{I_1} = 42$	98.1	Direct pairing: 2.846	$K_{c1} = 0.161$ $\tau_{I_1} = 94$	298.5	Direct pairing: -0.0746	Direct pairing: 0.1386
Loop 2, g_{22}	8.55	$K_{c2} = -11.87$ $\tau_{I_2} = 29$	33.6	Direct pairing: 2.977	$K_{c2} = 0.294$ $\tau_{I_2} = 64$	225.2		

In the Model 1 single-loop case, loop 2's LGC index is greater than loop 1. This indicates that a similar formula or rule tuned PI controller will perform better for loop 2 than loop 1. Note that the single-loop LGC value relies on the transfer function's time constant and delay. Because loop 2 has a lower delay-to-time constant ratio, it should be easier to regulate. Loop 2 has a higher maximum performance than loop 1. In closed-loop simulation of loops 1 and 2, the IAE value for the latter is smaller than the former, corroborating the LGC analysis conclusion. In Model 2, the single-loop case, loops 1 and 2 had lower LGC values than Model 1. This means that the step-down reaction controls the distillation process less than the step-up response. Closed-loop simulation verifies LGC analysis that Model 2's IAE values (loops 1 and 2) are bigger than Model 1. In addition, Model 2's LGC values for loops 1 and 2 are closer than Model 1, indicating that both loops should have better closed-loop performances. Again, the closed-loop simulation verifies this prediction, with Model 2's loop 2 to loop 1 IAE ratio of 0.9 and Model 1's 0.34. Closed-loop performance between loops improves as the ratio approaches unity.

In multi-loop, the LGC value depends on process time constants, delays, and diagonal RGA, therefore it accounts for process interaction. Table 5 shows the LGC values for loops 1 and 2 in the multi-loop situation (5^{th} order model) based on Model 1. The multi-loop example has lower LGC values for each loop than the single-loop case, indicating that the interaction effect reduces control performance. Loop 2 has a higher LGC value than loop 1, hence its closed-loop performance should be superior. This prediction is validated by the closed-loop simulation, where loop 2 has a lower IAE than loop 1. LGC analysis suggests that loops 1 and 2 will perform similarly because their LGC values are close. The closed-loop simulation under the multi-loop PI control scheme confirms this prediction, with loop 2's IAE ratio of 0.8 to loop 1.

Table 5: Distillation Column Step-Down Model 2: values of RGA, NI and LGC indices

Step Down Control Loop	**Single Loop: 1st Order Model**			**Multi-Loop: 5th Order (EOTF) Model**				
	LGC	PI controller	IAE	LGC	PI controller	IAE	RGA	NI
Loop 1, g_{11}	3.22	$K_{c1} = 0.538$ $\tau_{I_1} = 37$	140.6	Direct pairing: 3.111	$K_{c1} = 0.899$ $\tau_{I_1} = 46$	145.4	Direct pairing: 1.049	Direct pairing: 0.0936
Loop 2, g_{22}	4.84	$K_{c2} = -1.202$ $\tau_{I_2} = 69$	129.6	Direct pairing: 4.719	$K_{c2} = -1.293$ $\tau_{I_2} = 76$	138.6		

Model 2's step-down LGC computations result in a bigger discrepancy between loops 1 and 2's LGC values than Model 1. The distillation column's controllability is better with the step-down response than with the step-up response, unlike in the single-loop scenario where the LGC simply depends on the time constant and delay. The LGC depends on several time constants, delays, and the interaction impact in multi-loop cases.

Based on Models 1 and 2, the LGC index recommends direct pairings for decentralised control. However, Model 1 RGA analysis suggests indirect pairings because direct pairings lead to negative diagonal RGA components (Table 4). The NI index for direct pairings is quite low, suggesting indirect pairing is better. However, the closed-loop simulation in Figure 4 using Model 1 indicates that direct pairing works as anticipated by the LGC index, but indirect pairing fails to converge. When Model 2 is utilised, all indices suggest direct pairings. Loop 2 of both Model 1 and Model 2 has the best closed-loop performance, proving the LGC evaluation. This loop has bigger LGC values for both single-loop and multi-loop cases than loop 1.

3.1 Interacting Tanks

In this section, 4 interacting tanks (IT) is considered. Two tanks placed on top of another two tanks, where the objectives are to control the levels of the bottom tanks. The interacting tanks simulation was performed in the Control Station Loop Pro trainer software. Just like in the previous distillation column example, two linearized models are first obtained via step-up and step-down tests with similar perturbation magnitude, i.e., 10% of the nominal input value. The linearized model obtained by the step-up test is referred to as Model 3, and the model obtained via the step-down test is Model 4, as shown in Table 3. With regards to the single-loop case based on Model 3, Table 6 shows that the LGC value for loop 1 is larger than loop 2, which implies that loop 1 has a larger maximum achievable performance than loop 2. Based on Model 3 for the multi-loop case (refer to Table 6), the following observations can be made.

a) By comparing the LGC values for loops 1 and 2, the difference is about 20% under direct pairings and about 10% under indirect pairings. This means that the performance difference between loops 1 and 2 is larger under direct pairings than under indirect pairings. Closed-loop simulation confirms this prediction, where the difference in the IAE values of loops 1 and 2 is about 30% under direct pairings, while the difference is only about 10% under indirect pairings.
b) Under the direct/indirect pairing for loop 1, the difference between the IAE values of single-loop and multi-loop cases is about 5%. This result is within expectation since the difference in LGC values between the single-loop and multi-loop cases are quite small (about 10%). However, for loop 2 under direct pairings, the difference in IAE values between single-loop and multi-loop cases is larger, i.e., about 25% (the corresponding difference in the LGC values is about 20%). Thus, the smaller the LGC values between the single-loop and multi-loop cases of a given process, the smaller the difference between their IAE values.
c) While RGA and NI analyses result recommend only direct pairings, the LGC analysis suggests that either direct or indirect pairings are suitable for the interacting tanks. Certainly, indirect pairings can give a marked improvement in terms of the maximum achievable performances for loops 1 and 2. This result analysis is proven by the closed-loop simulation result, where the indirect pairings led to smaller IAE values than that of direct pairings.

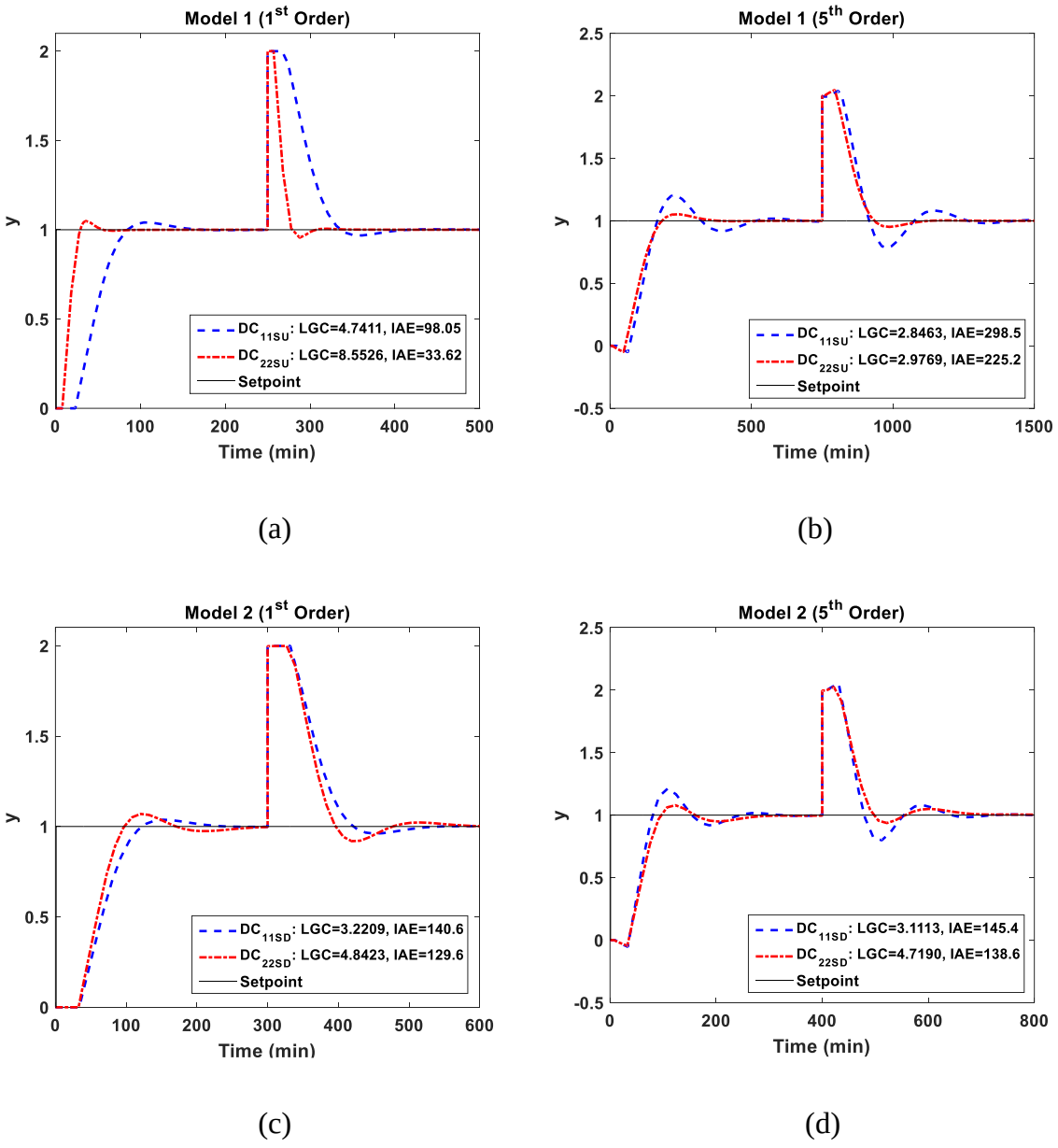

Figure 4: Closed-loop simulation of distillation using step-up and step-down models: a) single-loop Model 1 (Loop 1: DC_{11SU}, Loop 2: DC_{22SU}) b) multi-loop Model 1 (Loop 1: DC_{11SU}, Loop 2: DC_{22SU}), c) single-loop Model 2 (Loop 1: DC_{11SD}, Loop 2: DC_{22SD}), and d) multi-loop Model 2 (Loop 1: DC_{11SD}, Loop 2: DC_{22SD}).

Table 7 shows the LGC, RGA and NI values based on Model 4 (obtained by step-down test). The following observations are made.

a) When compared with the values in Table 6, it is obvious that the LGC values are markedly smaller for the multi-loop case, especially for loop 1 under direct or indirect pairings. However, loop 2 under the indirect pairings is an exception as both models lead to very comparable values. This means that Model 4 is more difficult to control than Model 3. Notice that the IAE values for both loops 1 and 2 under direct pairings in Table 7 are markedly larger than that in Table 6. This confirms that Model 4 has lower controllability properties than Model 3. The simulation results in Figure 5 show that for loop 2 under

indirect pairings, both multi-loop PI control of Model 3 and Model 4 lead to very close IAE values. This is in agreement with the LGC prediction.

b) It is observed that the difference in the LGC values between the single-loop case and the multi-loop case is substantial. As the latter shows smaller LGC values than the former, the interaction effect is more substantial in Model 4. However, little change is observed in the values of RGA and NI indices (see Tables 6 and 7). In other words, both RGA and NI analyses do not show a substantial difference between the controllability property of Model 4 and Model 3. Therefore, the LGC index successfully provides a more accurate measure of controllability properties than both the RGA and NI indexes.

Table 6: Interacting Tanks Step-Up Model 3: values of RGA, NI and LGC indices.

Step-Up Control Loop	**Single Loop: 1st Order Model**			**Multi-Loop: 5th Order (EOTF) Model**				
	LGC	PI controller	IAE	LGC	PI controller	IAE	RGA	NI
Loop 1, g_{11}	6.550	$K_{c1} = 19.7$ $\tau_{I_1} = 16$	24.8	Direct pairing: 5.1067 Indirect pairing: 5.3921	Direct pairing: $K_{c11} = 37.62$ $\tau_{I_{11}} = 28$ Indirect pairing: $K_{c21} = -10.13$ $\tau_{I_{21}} = 16$	Direct pairing: 26.2 Indirect pairing: 25.9	Direct pairing: 1.3547	Direct pairing: 0.5237
Loop 2, g_{22}	5.254	$K_{c2} = 18.8$ $\tau_{I_2} = 14$	25.7	Direct pairing: 4.017 Indirect pairing: 5.9012	Direct pairing: $K_{c22} = 21.73$ $\tau_{I_{22}} = 18$ Direct pairing: $K_{c12} = -13.22$ $\tau_{I_{12}} = 18$	Direct pairing: 34.19 Indirect pairing: 28.7		

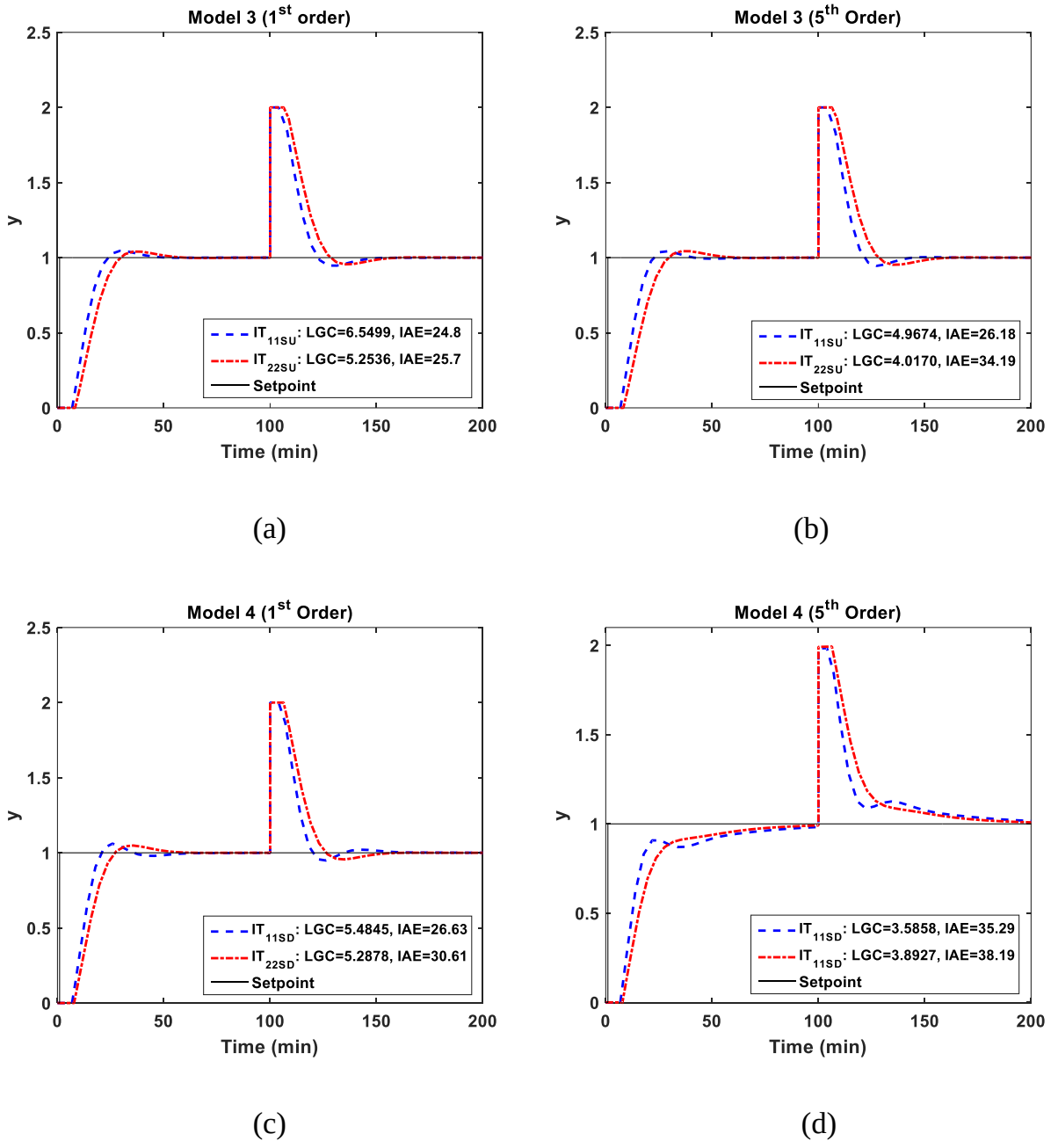

Figure 5: Closed-loop simulation of interacting tanks using step-up and step-down models: a) single-loop Model 3 (Loop 1: IT_{11SU}, Loop 2: IT_{22SU}) b) multi-loop Model 3 (Loop 1: IT_{11SU}, Loop 2: IT_{22SU}), c) single-loop Model 4 (Loop 1: IT_{11SD}, Loop 2: IT_{22SD}), and d) multi-loop Model 2 (Loop 1: IT_{11SD}, Loop 2: IT_{22SD}).

Table 7: Interacting Tanks Step-Down Model 4: values of RGA, NI and LGC indices.

Step Down Control Loop	**Single Loop: 1st Order Model**			**Multi-Loop: 5th Order (EOTF) Model**				
	LGC	PI controller	IAE	LGC	PI controller	IAE	RGA	NI
Loop 1, g_{11}	5.484	$K_{c1} = 19.50$ $\tau_{I_1} = 15$	26.6	Direct pairing: 3.586 Indirect pairing: 4.4054	Direct pairing: $K_{c11} = 28.12$ $\tau_{I_{11}} = 24$ Indirect pairing: $K_{c21} = -10.95$ $\tau_{I_{21}} = 13$	Direct pairing: 35.3 Indirect pairing: 27.1	Direct pairing: 1.4141	Direct pairing: 0.5857
Loop 2, g_{22}	5.288	$K_{c2} = 14.81$ $\tau_{I_2} = 14$	30.61	Direct pairing: 3.893 Indirect pairing: 5.9012	Direct pairing: $K_{c22} = 19.95$ $\tau_{I_{22}} = 19$ Indirect pairing: $K_{c12} = -12.22$ $\tau_{I_{12}} = 14$	Direct pairing: 38.2 Indirect pairing: 30.6		

4. Case Study: Sulfuric Acid Decomposition of Renewable Hydrogen Production Process

4.1 Process Description

The sulfuric acid decomposition section (Section II) of the Sulfur-Iodine Thermochemical Cycle (SITC) process for hydrogen production [20] has received insufficient attention in the design, control and simulation. Due to the high energy requirement, the requisite energy for this reactor is typically derived from an external high-temperature reactor, such as a nuclear reactor or solar energy [21, 22]. This creates significant challenges concerning the control and operation of the SITC plant and contributed to several investigations [15–18] on the behaviour of Section II. In this work, a sulfuric acid decomposition reactor of the SITC plant named the Sulfuric Acid-Integrated Boiler Superheater Decomposer (SA-IBSD) reactor is developed as depicted in Figure 6. The SA-IBSD reactor was developed based on a patented bayonet reactor by Moore et.al, (2011) [23]. The patented reactor is designed to conduct exceptionally endothermic reactions at temperatures up to 950°C, which is suitable for the SA-IBSD reactor reaction. The design of the bayonet reactor uses a comparable concept of both a heat exchanger and a packed bed reactor. Inside the shell of the industrial-scale reactor, there are several tubes, a catalyst section and a manifold.

4.2 Controllability Analysis

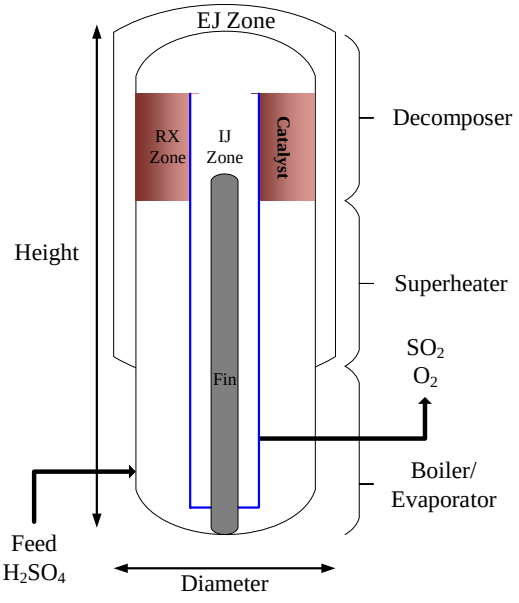

Figure 6: Schematic diagram of a single-tube SA-IBSD reactor.

As the SA-IBSD reactor is a rigid process, the ode15s solver in MATLAB is utilised for the simulation of the first principle model and its validation. Table 8 lists four linearized models of the SA-IBSD reactor generated under various operating conditions. Table 9 displayed the LGC score for models P1, P2, P3, and P4. Table 9's RGA and NI values indicate that the SA-IBSD process has little interaction among its variables, suggesting that direct coupling is the most effective method for controlling it.

Based on LGC analysis, how well does this pairing perform? First, the 1st and 5th-order controllers' LGC values should be equal to compare their performance. Second, positive 1st and 5th-order LGC indicators indicate a controllable pairing. Table 9 shows that all models exhibit positive LGC and are controllable. Thirdly, a low LGC score (near to 1) may indicate poor controllability, and vice versa. Table 9 of the 5th-order model shows that model P4 has a low LGC value, suggesting poor controllability, while model P2 has the highest LGC value, indicating optimal controllability.

Table 8: Linearized models of SA-IBSD reactor at four different operating conditions.

No	Model	Operating Condition
1	$\mathbf{P1} = \begin{bmatrix} \frac{-0.0225e^{-8.92s}}{1.35s+1} & \frac{7.03x10^{-7}e^{-8.3s}}{0.03s+1} \\ \frac{-1.35x10^{3}e^{-9.26s}}{0.69s+1} & \frac{1.55e^{-2.7s}}{4.5x10^{-5}s+1} \end{bmatrix}$	25% increase in nominal feed pressure
2	$\mathbf{P2} = \begin{bmatrix} \frac{-2.29e^{-8.92s}}{1.35s+1} & \frac{7.03x10^{-7}e^{-8.3x10^{-3}s}}{0.03s+1} \\ \frac{-1.64x10^{4}e^{-9.26s}}{0.69s+1} & \frac{1.55e^{-2.7x10^{-3}s}}{4.5x10^{-5}s+1} \end{bmatrix}$	25% decrease in nominal feed temperature
3	$\mathbf{P3} = \begin{bmatrix} \frac{-0.0225e^{-8.92s}}{1.35s+1} & \frac{7.1x10^{-3}e^{-9.3s}}{0.03s+1} \\ \frac{-1.35x10^{3}e^{-9.26s}}{0.69s+1} & \frac{9705e^{-2.7s}}{4.5x10^{-5}s+1} \end{bmatrix}$	25% decrease in nominal feed flow rate
4	$\mathbf{P4} = \begin{bmatrix} \frac{-2.29e^{-8.92s}}{1.35s+1} & \frac{7.03x10^{-6}e^{-8.3x10^{-3}s}}{0.03s+1} \\ \frac{2.35x10^{6}e^{-9.26s}}{0.69s+1} & \frac{1.61e^{-2.7x10^{-3}s}}{4.5x10^{-5}s+1} \end{bmatrix}$	25% increase in nominal external jacket temperature

Table 9: Indicators of LGC, RGA and NI controllability analysis for various systems.

Model	Single Loop: 1st Order Model			Multi-Loop: 5th Order (EOTF) Model				
	LGC	PI controller	IAE	LGC	PI controller	IAE	RGA	NI
P1	1.3027	$\boldsymbol{K_{c1} = 0.021177}$ $\boldsymbol{\tau_{I_1} = 1}$	42.55	1.3956	$\boldsymbol{K_{c1} = -3.329}$ $\boldsymbol{\tau_{I_1} = 0.769}$	38.6	1.028	U1-Y1 8.7×10^{-5}
P2	1.3027	$\boldsymbol{K_{c1} = 0.021177}$ $\boldsymbol{\tau_{I_1} = 1}$	42.55	1.4488	$\boldsymbol{K_{c1} = -0.0416}$ $\boldsymbol{\tau_{I_1} = 0.588}$	37.8	1.003	U1-Y1 6.5×10^{-4}
P3	1.3027	$\boldsymbol{K_{c1} = 0.021177}$ $\boldsymbol{\tau_{I_1} = 1}$	42.55	1.4011	$\boldsymbol{K_{c1} = -3.1279}$ $\boldsymbol{\tau_{I_1} = 0.8333}$	38.5	1.0454	U1-Y1 8.69×10^{-2}
P4	1.3027	$\boldsymbol{K_{c1} = 0.021177}$ $\boldsymbol{\tau_{I_1} = 1}$	42.55	1.0838	$\boldsymbol{K_{c1} = -0.00327}$ $\boldsymbol{\tau_{I_1} = 0.769}$	88.7	-0.287	U1-Y2 4.4×10^{-3}

The P2 controller parameters are selected, implemented, and assessed for the nonlinear dynamic model. Figure 7 shows sustained oxygen and temperature outputs. Comparing the newly proposed LGC approach to the existing controllability indices such as RGA and NI [3, 19], LGC successfully recognised system stability and controllability. Not only did it take fewer steps, but it also estimated controller performance well.

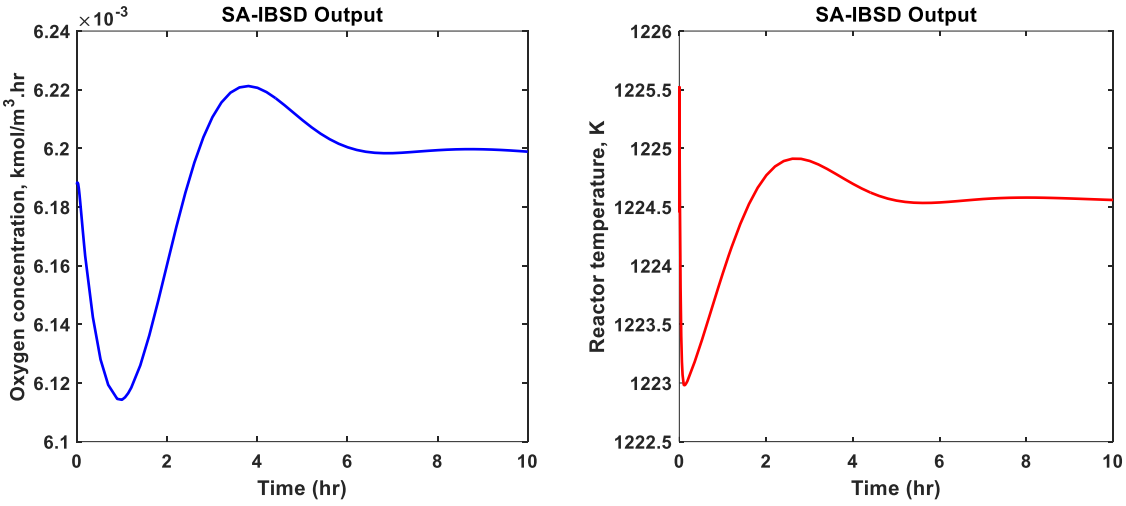

(a) (b)

Figure 7: SA-IBSD reactor outputs for nonlinear system (setting model P2 of Table 9) controlled by PI controller: (a) Oxygen concentration, and (b) Temperature.

Conclusion

As an alternative controllability index, a comprehensive LGC method that simplify the controllability evaluation task has been put forward in this work. The index assesses the effect of process interaction, deadtimes, and time constants on the optimum controllability performance that can be attained. In addition to providing an evaluation of potential pairings, this method may additionally predict the controller performance attainable from any particular pairing. The LGC index is not only capable to identify the controllability but the stability of a particular designed control system. The primary advantage of the presented LGC method is that it makes simpler the controllability evaluation task by replacing the use of a small number of controllability indices with a single LGC method to determine the pairing and controllability performance of the desired TITO process. This greatly simplifies an otherwise extremely intricate decentralised PID control tuning resulting from process interactions. Despite its benefits, it should be emphasised that the LGC has drawbacks, as the total time delays of the system of interest must be greater than zero, $\theta_{I_i} > 0$. To further develop the LGC's potential so that it can serve as a practical controllability analysis index, more LGC tests specifically on nonlinear chemical processes needs to be conducted in the future.

Acknowledgments

The financial support from Xiamen University Malaysia through the XMUM Research Fund (XMUMRF/2021-C7/IENG/0035), FRGS grant (no: JPT.S Jld.13(28)) of Ministry of Higher Education (MOHE), and a CSRI grant of Curtin University Sarawak and are greatly acknowledged.

References

[1] E. H. Bristol, "New Measure of Interaction for Multivariable Process Control," IEEE Transaction Automatica Control, no. AC-11, pp. 133–134, 1966.

[2] A. Niederlinski, "A heuristic approach to the design of linear multivariable interacting control systems," Automatica, vol. 7, no. November 1970, pp. 691–701, 1971, doi: 10.1016/0005-1098(71)90007-0.

[3] G. Karami, M. Amidpour, B. H. Sheibani, and G. R. Salehi, "Distillation column controllability analysis through heat pump integration," Chemical Engineering and Processing: Process Intensification, vol. 97, pp. 23–37, 2015, doi: 10.1016/j.cep.2015.08.005.

[4] W. Chin, H. Song, J. H. Lee, and D. Ramkrishna, "Control Engineering Practice Hybrid cybernetic model-based simulation of continuous production of lignocellulosic ethanol : Rejecting abruptly changing feed conditions," Control Engineering Practice, vol. 18, no. 2, pp. 177–189, 2010, doi: 10.1016/j.conengprac.2009.09.002.

[5] J. B. Froisy, "Model predictive control — Building a bridge between theory and practice," vol. 30, no. May, pp. 1426–1435, 2006, doi: 10.1016/j.compchemeng.2006.05.044.

[6] N. Mohd and N. Aziz, "Performance and robustness evaluation of Nonlinear Autoregressive with Exogenous input Model Predictive Control in controlling industrial fermentation process," Journal of Cleaner Production, vol. 136, pp. 42–50, 2016, doi: 10.1016/j.jclepro.2016.06.191.

[7] L. Alberto, P. Suárez, P. Georgieva, S. Feyo, and D. Azevedo, "Chemical Engineering Research and Design Nonlinear MPC for fed-batch multiple stages sugar crystallization," vol. 9, no. February, pp. 753–767, 2010, doi: 10.1016/j.cherd.2010.10.010.

[8] G. Shafiee, M. M. Arefi, M. R. Jahed-Motlagh, and A. A. Jalali, "Nonlinear predictive control of a polymerization reactor based on piecewise linear Wiener model," Chemical Engineering Journal, vol. 143, no. 1–3, pp. 282–292, 2008, doi: 10.1016/j.cej.2008.05.013.

[9] G. P. Rangaiah and V. Kariwala, Plantwide Control Recents Developments and Applications, First. United Kingdom: John Wiley and Sons Ltd, 2012.

[10] Y. Shen, W. Cai, and S. Li, "Multivariable Process Control: Decentralized, Decoupling, or Sparse?," no. 2, pp. 761–771, 2010.

[11] N. Mohd, J. Nandong, S. R. Abd Shukor, W. Y. Ong, K. W. Tan, and S. A. Sirajul Adly, "Dynamic Modelling and Process Control of Iodine-Sulfur Thermochemical Cycle for Hydrogen Production: A Bibliometric Study and Research Prospect," Arch. Comput. Methods Eng., 2023, doi: 10.1007/s11831-023-09988-9.

[12] Q. H. Seer and J. Nandong, "Stabilization and PID tuning algorithms for second-order unstable processes with time-delays," ISA Transactions, vol. 67, pp. 233–245, 2017.

[13] Q. H. Seer and J. Nandong, "Stabilising PID tuning for a class of fourth-order integrating nonminimum-phase systems.," International Journal of Control, pp. 1–17, 2017.

[14] R. K. Pearson, "Selecting nonlinear model structures for computer control," vol. 13, pp. 1–26, 2003.

[15] H. Noguchi, A. Terada, K. Onuki, and R. Hino, "Boiling heat transfer characteristics of a sulfuric-acid flow in thermochemical iodine–sulfur cycle," Chemical Engineering Research and Design, vol. 92, no. 9, pp. 1659–1663, 2014, doi: 10.1016/j.cherd.2013.12.014.

[16] Y. S. Kim, H. C. No, J. Y. Choi, and H. J. Yoon, "Stability and kinetics of powder-type and pellet-type iron (III) oxide catalysts for sulfuric acid decomposition in practical Iodine-Sulfur cycle," Int J Hydrogen Energy, vol. 38, no. 9, pp. 3537–3544, 2013, doi: 10.1016/j.ijhydene.2013.01.039.

[17] J. Park, J. H. Cho, H. Jung, K. D. Jung, S. Kumar, and I. Moon, "Simulation and experimental study on the sulfuric acid decomposition process of SI cycle for hydrogen production," Int J Hydrogen Energy, vol. 38, no. 14, pp. 5507–5516, 2013, doi: 10.1016/j.ijhydene.2013.03.027.

[18] S. N. Rashkeev, D. M. Ginosar, L. M. Petkovic, and H. H. Farrell, "Catalytic activity of supported metal particles for sulfuric acid decomposition reaction," Catal Today, vol. 139, no. 4, pp. 291–298, 2009, doi: 10.1016/j.cattod.2008.03.029.

[19] Y. Shen, W. Cai, and S. Li, "Multivariable Process Control: Decentralized, Decoupling, or Sparse?," no. 2, pp. 761–771, 2010.

[20] L. C. Juárez-Martínez, G. Espinosa-Paredes, A. Vázquez-Rodríguez, and H. Romero-Paredes, "Energy optimization of a Sulfur–Iodine thermochemical nuclear hydrogen production cycle," Nucl. Eng. Technol., vol. 53, no. 6, pp. 2066–2073, 2021, doi: 10.1016/j.net.2020.12.014.

[21] N. Hiroki et al., "Hydrogen production using thermochemical water-splitting Iodine–Sulfur process test facility made of industrial structural materials: Engineering solutions to prevent iodine precipitation," Int. J. Hydrogen Energy, vol. 46, no. 43, pp. 22328–22343, 2021.

[22] Q. Wang, C. Liu, D. Li, and R. Macián-Juan, "Optimization and comparison of two improved very high temperature gas-cooled reactor-based hydrogen and electricity cogeneration systems using iodine-sulfur cycle," Int. J. Hydrogen Energy, vol. 47, no. 33, pp. 14777–14798, 2022, doi: 10.1016/j.ijhydene.2022.02.237.

[23] R. Moore, P. S. Pickard, E. J. Pharma Jr, M. E. Vernon, F. Gelbard, and R. X. Lenard, "United States Patent: Integrated Boiler, Superheater and Decomposer for Sulfuric Acid Decomposition," vol. 2, no. 12, pp. 19–35, 2011, doi: 10.1145/634067.634234.

APPENDIX

Consider the $2x2$ (TITO) process given by

$$\mathrm{P(s)} = \begin{bmatrix} \mathrm{g_{11}(s)} & \mathrm{g_{12}(s)} \\ \mathrm{g_{21}(s)} & \mathrm{g_{22}(s)} \end{bmatrix} \tag{11}$$

where the transfer function g_{ij} for $i = 1, 2$ and $j = 1, 2$ takes the FOPDT form

$$g_{ij}(s) = \frac{k_{ij}\, exp(-\theta_{ij}s)}{\tau_{ij}s+1} \tag{12}$$

The k_{ij}, τ_{ij} , and θ_{ij} represent the process gain, the time constant, along with the deadtime, correspondingly, in equation (6). Prior to deriving the LGC index, it is necessary to transform the transfer function matrix (5) to the decoupled form shown below:

$$P(s) = \begin{bmatrix} g_1^{eff}(s) & 0 \\ 0 & g_2^{eff}(s) \end{bmatrix} \tag{13}$$

The decoupled effective open-loop transfer function (EOTF) in (7) is given by

$$\boldsymbol{g_i^{eff}(s) = g_{ii}(s) - \frac{g_{ij}(s)g_{ji}(s)}{g_{jj}(s)}} \tag{14}$$

Upon simplification, the EOTF (8) can be expressed in the following form

$$\boldsymbol{g_i^{eff}(s) = k_{ii}\left[\frac{exp(-\theta_{ii}s)}{\tau_{ii}s+1} - \left(\frac{k_{ij}k_{ji}}{k_{ii}k_{jj}}\right)\left(\frac{(\tau_{jj}s+1)\, exp(-\theta_{I_i}s)}{(\tau_{ij}s+1)(\tau_{ji}s+1)}\right)\right]} \tag{15}$$

where effective deadtime is $\theta_{I_i} = \theta_{ij} + \theta_{ji} - \theta_{jj}$.

One can further express (9) in terms of the diagonal RGA element, e.g., λ_{11}, thus giving

$$g_1^{eff}(s) = k_{11}\left[\frac{exp(-\theta_{11}s)}{\tau_{11}s+1} - \psi_1\left(\frac{(\tau_{22}s+1)\, exp(-\theta_{I_1}s)}{(\tau_{12}s+1)(\tau_{21}s+1)}\right)\right] \tag{16}$$

In equation (10), ψ_1 is defined as

$$\psi_1 = \frac{k_{12}k_{21}}{k_{11}k_{22}} = \frac{\lambda_{11}-1}{\lambda_{11}} \tag{17}$$

The RGA matrix λ corresponding to (11) assumes direct pairings are adopted, where

$$\lambda = \begin{bmatrix} \lambda_{11} & 1-\lambda_{11} \\ 1-\lambda_{11} & \lambda_{11} \end{bmatrix} \quad (18)$$

and

$$\lambda_{11} = \frac{k_{11}}{k_{11} - \frac{k_{12}k_{21}}{k_{22}}} \quad (19)$$

The maximum lower limit and the minimum upper limit can be obtained by solving equations as follows,

Equation (12) can be simplified into a polynomial form. The LGC equations are modelled in the MATLAB environment.

$$f_6 s^6 + (f_5 + K_{L_1} h_5) s^5 + (f_4 + K_{L_1} h_4) s^4 +$$
$$(f_3 + K_{L_3} h_3) s^3 + (f_2 + K_{L_2} h_2) s^2 +$$
$$(f_1 + K_{L_1} h_1) s + K_{L_1} h_0 = 0$$

Given that,

$f_6 = a_4 \tau_{11} \tau_{I_1}$
$f_5 = (a_3 \tau_{11} + a_4) \tau_{J_1}$
$f_4 = (a_2 \tau_{11} + a_3) \tau_{I_1}$
$f_3 = (a_1 \tau_{11} + a_2) \tau_{I_1}$
$f_2 = (\tau_{11} + a_1) \tau_{I_1}$
$f_1 = \tau_{I_1}$

General equation,

$f_k = (a_{k-2} \tau_{11} + a_{k-1}) \tau_{I_1} \quad for\ k = 1,2,\dots,6$
$h_5 = \tau_{I_1} (b_{14} - \psi_1 b_{24})$
$h_4 = \tau_{I_1} (b_{13} - \psi_i b_{23}) + b_{14} - \psi_1 b_{24}$
$h_3 = \tau_{I_1} (b_{12} - \psi_1 b_{22}) + b_{13} - \psi_1 b_{23}$
$h_2 = \tau_{I_1} (b_{11} - \psi_1 b_{21}) + b_{12} - \psi_1 b_{22}$
$h_1 = \tau_{I_1} (b_{10} - \psi_1 b_{20}) + b_{11} - \psi_1 b_{21}$
$h_0 = 1 - \psi_1$

General equation

$h_k = \tau_{I_1} (b_{1(k-1)} - \psi_1 b_{2(k-1)}) + b_{1k} - \psi_1 b_{2k}$
$for\ k = 0.1,\dots,5$

The parameters definition in equations (14) and (15) are as follows,

$a_{-1} = 0$
$a_0 = 1$
$a_1 = \tau_{12} + \tau_{21} + \alpha_{11} + \alpha_{I_1}$
$a_2 = \tau_{12}\tau_{21} + (\tau_{12} + \tau_{21})(\alpha_{11} + \alpha_{I_1}) + \alpha_{11}\alpha_{I_1}$
$a_3 = \tau_{12}\tau_{21}(\alpha_{11} + \alpha_{I_1}) + \alpha_{11}\alpha_{I_1}(\tau_{12} + \tau_{21})$
$a_4 = \tau_{12}\tau_{21}\alpha_{11}\alpha_{I_1}$
$b_{1(-1)} = b_{2(-1)} = 0$
$b_{10} = b_{20} = 1$
$b_{11} = \alpha_{I_1} - \alpha_{11} + \tau_{12} + \tau_{21}$
$b_{12} = -\alpha_{11}\alpha_{I_1} + (\alpha_{I_1} - \alpha_{11})(\tau_{12} + \tau_{21}) + \tau_{12}\tau_{21}$
$b_{13} = -\alpha_{11}\alpha_{I_1}(\tau_{12} + \tau_{21}) + (\alpha_{I_1} - \alpha_{11})\tau_{12}\tau_{21}$
$b_{14} = -\alpha_{11}\alpha_{I_1}\tau_{12}\tau_{21}$
$b_{21} = \tau_{11} + \tau_{22} + \alpha_{11} - \alpha_{I_1}$
$b_{22} = \tau_{11}\tau_{22} + (\tau_{11} + \tau_{22})(\alpha_{11} - \alpha_{I_1}) - \alpha_{11}\alpha_{I_1}$
$b_{23} = \tau_{11}\tau_{22}(\alpha_{11} - \alpha_{I_1}) - \alpha_{11}\alpha_{I_1}(\tau_{11} + \tau_{22})$
$b_{24} = -\tau_{11}\tau_{22}\alpha_{11}\alpha_{I_1}$

The condition for P-controller,

$$\left.\begin{matrix} K_{upper\ k} = \frac{(a_{k-1}\tau_{11}+a_k)}{|f_k|} \\ K_{lower\ k} = -inf \end{matrix}\right\} if\ f_k < 0, for\ k = 1,2,3,4$$

$$\left.\begin{matrix} K_{upper\ k} = \frac{-(a_{k-1}\tau_{11}+a_k)}{f_k} \\ K_{lower\ k} = -inf \end{matrix}\right\} if\ f_k > 0, for\ k = 1,2,3,4$$

The condition for PI controller,

$$\left.\begin{matrix} K_{upper\ k} = \frac{(a_{k-2}\tau_{11}+a_{k-1})\tau_{I_1}}{|f_k|} \\ K_{lower\ k} = -inf \end{matrix}\right\} if\ f_k < 0, for\ k = 1,2,3,4,5,6$$

$$\left.\begin{matrix} K_{upper\ k} = \frac{-(a_{k-2}\tau_{11}+a_{k-1})\tau_{I_1}}{f_k} \\ K_{lower\ k} = -inf \end{matrix}\right\} \text{if } f_k > 0, \text{for k} = 1,2,3,4,5,6$$

Finally, the limit or stability region can be calculated

$$\overline{K}_{min} = \min\left(K_{upper\ k}\right)$$

$$\underline{K}_{max} = \max\left(K_{lower\ k}\right)$$

By providing three desired inputs; process gains, time constants and time delays, one may calculate the limits ($\overline{K}_{min}$ and $\underline{K}_{max}$) via a designed m-file in the Matlab software.